Supporting Information

Visualized Simulation for Nanotructural Design of Flexible Strain Sensors: from Numerical Model to Experimental Verification

Jize Liu, Fengyuan Zhao, Qingchuan Tao, Jie Cao, Yanmei Yu, Xinxing Zhang*

[a].State Key Laboratory of Polymer Materials Engineering, Polymer Research Institute of Sichuan University, Chengdu 610065, China

[b].College of Electronics and Information Engineering, Sichuan University, Chengdu 610065, China

*Corresponding author: Xinxing Zhang. E-mail address: xxzwwh@scu.edu.cn

Tel: +86-28-85460607 Fax: +86-28-85402465

Experimental Section

Materials: Natural rubber (NR) latex (solid content: 58.0 wt%) was supplied by the Agricultural Products Processing Research Institute, Chinese Academy of Tropical Agricultural Science, Zhanjiang, P. R. China. Cotton cellulose was subjected to cutting and shredding processes and then used without further purification or bleaching. Multiwall carbon nanotubes (CNTs, >95%), with a mean diameter of d=10-20 nm and a length of L=10-30 μm, were obtained from Chengdu Organic Chemicals Co., Ltd Chinese Academy of Sciences. Sulfuric acid (95−98%) was supplied by Kelong Chemical Regent Co., Ltd. (Chengdu, China). All chemical materials and solvents used in the experiments were analytical grade reagents and were used without further purification.

Preparation of CNTs@CNC nanohybrids: Cellulose nanocrystals (CNC) were prepared by controlled acid hydrolysis of cotton fibers. The CNTs@CNC nanohybrids were synthesized by an ultrasonically assisted mixing process. 0.08 g of CNTs were added into a well-dispersed aqueous solution of CNCs (containing 0.08 g of CNC, 500 mL). The mixture was sonicated for 10 min (1200 W) at room temperature to obtain a uniform CNTs@CNC nanohybrid suspension.

Preparation of CNTs@CNC/NR composites with 3D segregated structure: The CNTs@CNC/NR nanocomposites with 3D segregated structure were prepared according to the following procedures. The desired amount of pre-dispersed CNTs@CNC nanohybrid suspension and NR latex was mixed uniformly under mild magnetic stirring. For the composites with different volume fractions of CNTs, we kept

the amount of NR latex fixed at 0.17 g (containing 0.1 g of NR) and varied the amount of CNTs@CNC nanohybrid suspension. Then we prepared mixed suspensions with five different volume fractions of CNTs, i.e., 1.2, 2.0, 2.8, 3.5 and 4.2, respectively. Then a thin layer of the composites with 3D segregated structure were coated on NR substrate via drop-casting (demulsificated by hydrochloric acid) and followed by drying in an electric oven for the following conductivity and sensitivity measurements.

Preparation of randomly dispersed CNTs/NR nanocomposites: The samples of CNTs/NR nanocomposites without the addition of CNC were prepared by two-roll mill mixing to form a homogeneously dispersed morphology. For the composites with different volume fractions of CNTs, we kept the amount of NR fixed at 20 g and varied the amount of CNTs powder to obtain composites with seven different volume fractions of CNTs, i.e., 4, 5, 6, 7, 8, 9 and 10, respectively.

Preparation of nanocomposites with multilayer structure: At first, 1 g chitosan was dissolved in 100 mL, 1 wt% concentration of acetic acid solution to obtain chitosan solutions (chitosan: 1 wt%). 9 g CT solution was mixed with NR latex (6.89 g, solid content: 58.0 wt%) with stirring for 10 min, then the obtained suspension was dilution into 10 times to obtain the chitosan/NR hybrids (chitosan@NR) suspension.Then the obtained CNTs@CNC suspension (CNTs: 0.08 g/500 mL) and chitosan@NR suspension were sprayed onto the surface of NR substrate and dried in a blast oven (60 ºC) alternately. As a result, the CNTs and chitosan form thin layers alternately and set up a controllable multilayer structure.

Characterization: Zeta potential values of the suspensions and solutions were measured using Zetasizer nano-ZS (Malvern, UK). The morphology of CNTs@CNC nanohybrids and the interfacial morphology of CNTs@CNC/NR nanocomposites were observed by transmission electron microscope (JEOL JEM-100CX, Japan) and scanning electron microscope (JSM-5600, JEOL, Japan). The electric resistance of all samples was measured by a two-point measurement with a resistance meter (UT61, Uni-trend, China). The mechanical property and sensitivity were measured using a universal tensile testing machine (Instron-5560, USA) with an extension rate of 10 mm/min at room temperature. The 50 000 cycles of bending were proceeded in a multifunction oscillator (HY-3A, Ronghua, China). The sensing performances of all strain sensors were measured in real-time by a two-point measurement with a Keithley 2601B source meter (USA).

A 3D unit cell was constructed as shown in **Figure 1a**, and rubber spheres were set in the unit cell as follows:

$$(x - a)^2 + (y - b)^2 + (z - c)^2 = R^2 \tag{S1}$$

Where (a, b, c) is the spatial coordinates of the centre of spheres, R is the radius (0.5 μm in this system). Then CNTs should be set in a special way to fit the facts as follows: the start point was set by the rand function in Matlab software:

$$Start\ point = (rand * Lx, rand * Ly, rand * Lz) \tag{S2}$$

The directional vector u was set randomly, then the end point was calculated:

$$End\ point = s + \left(L / sqrt(u * u') \right) * u \tag{S3}$$

Where L is the length of CNTs. These formulas ensured the stochastic dispersion of CNTs, however, due to the physical constraint of these nanostructures, there were some inconsequent CNTs (for example, the CNTs located outside the 3D cube or contacted with each other) should be removed and replaced. And for 3D segregated structure ("Seg"), CNTs passed through or contacted with rubber spheres should also be replaced to ensure the rationality of 3D segregated conductive network in restricted space. For multilayer structure ("Mul"), the z coordinates of start points and end points were set to determined values and then varied the z values to obtain different layers.

Table S1. Detailed parameters in the unit cell.

Unit cell	Spatial size (Length * width * height)	Number of CNTs	Number of CNTs in pathes	Number of tunnel nodes
Seg-1.6	2.1 μm*2.1 μm*2.1 μm	858	596	1430
Seg-1.8	2.1 μm*2.1 μm*2.1 μm	965	702	1715
Seg-2.0	2.1 μm*2.1 μm*2.1 μm	1088	871	2218
Seg-2.4	2.1 μm*2.1 μm*2.1 μm	1286	1117	3099
Seg-2.8	2.1 μm*2.1 μm*2.1 μm	1500	1331	3943
Seg-3.2	2.1 μm*2.1 μm*2.1 μm	1715	1621	5197
Ran-5	1.05 μm*1.05 μm*1.05 μm	835	516	1166
Ran-6	1.05 μm*1.05 μm*1.05 μm	1002	795	1220
Ran-7	1.05 μm*1.05 μm*1.05 μm	1169	1021	2800
Ran-8	1.05 μm*1.05 μm*1.05 μm	1336	1203	3459
Ran-9	1.05 μm*1.05 μm*1.05 μm	1503	1395	4489
Ran-10	1.05 μm*1.05 μm*1.05 μm	1670	1599	5507
Mul	10 μm*2.5 μm*10 nm	500	496	1795

In the systems, CNTs with with a diameter of d=10 nm (given in the specification of our CNTs), rubber spheres with a diameter of R=1μm according to the TEM imagines. For the numerical simulation of multilayer structure and 3D segregated structure, the length of CNTs was set as 1 μm according to the TEM imagines, and 0.4 μm for randomly dispersed structure attributed to the strong shear action under two-roll milling. The number of CNTs is calculated according to the volume fraction (for Mul structure, the number was determined according to the volume ration of CNTs and CNC), and the cut off distance of tunnel is determined according to relative works.[1,2]
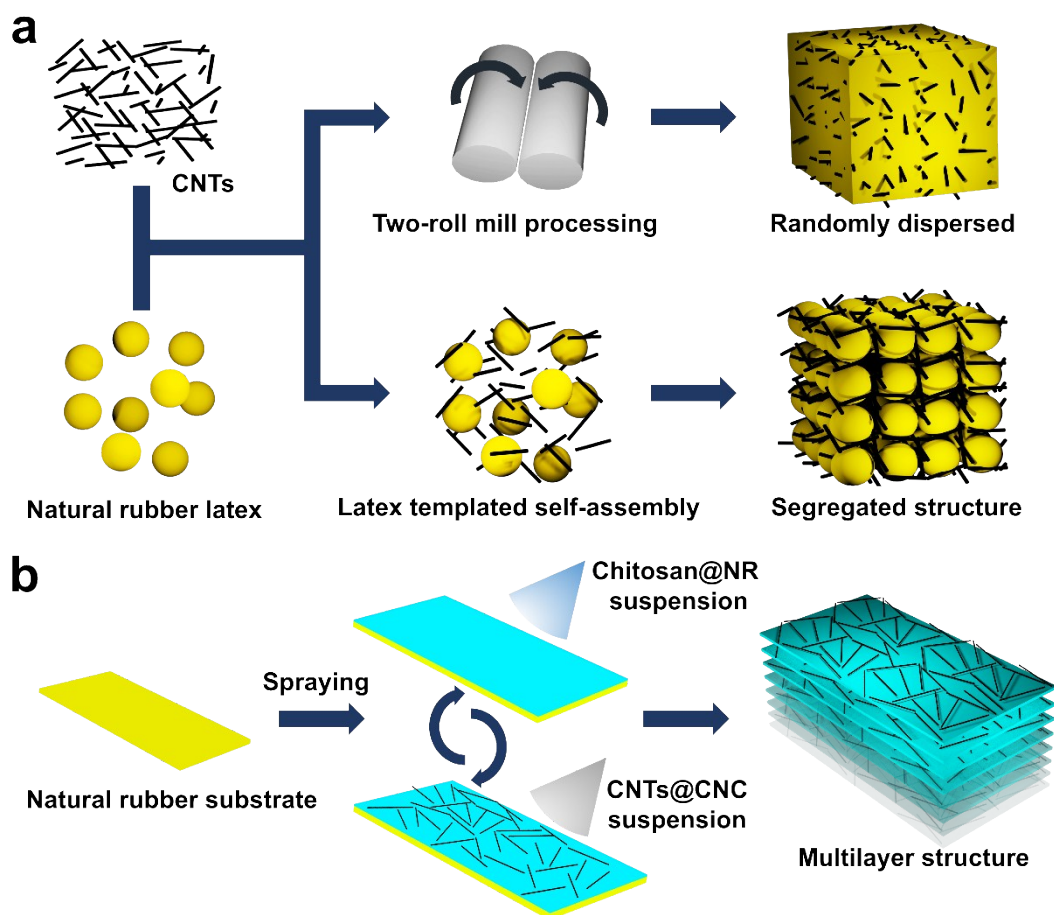
Figure S1. Schematic illustration for the fabrication of composites with (a) randomly dispersed structure (Ran), 3D segregated structure (Seg) and (b) multilayer structure (Mul).

The randomly dispersed structure was fabricated by two-roll mill mixing without any complex nanostructure control. In order to achieve "Seg" and "Mul" structure, specific fabricating process are needed. At first, carbon nanotubes (CNTs) were steadily dispersed into water by the effect of amphiphilic cellulose nanocrystals (CNC) as shown in **Figure S2** and **S3**. Attributed to the excluded volume effect of natural rubber (NR) rubber latex particles and the unique amphiphilicity of CNTs@CNC nanohybrids, CNTs were pushed into the interstitial space between rubber latex particles and form a 3D segregated conductive network during the coagulation process. As for multilayer

structure, as illustrated in **Figure S1b** and **S4**, CNTs suspension and chitosan@NR suspension was sprayed alternately onto the surface of rubber substrate and dried in a blast oven. Attributed to the electrostatic interaction between CNTs/CNC nanohybrids with negative charge and chitosan@NR suspension with positive charge, CNTs and chitosan@NR hybrids formed thin layers alternately and set up a controllable multilayer structure. For the numerical simulation of multilayer structure and 3D segregated structure, the length of CNTs was set as 1 μm according to the TEM imagines, and 0.4 μm for randomly dispersed structure attributed to the strong shear action under two-roll milling.
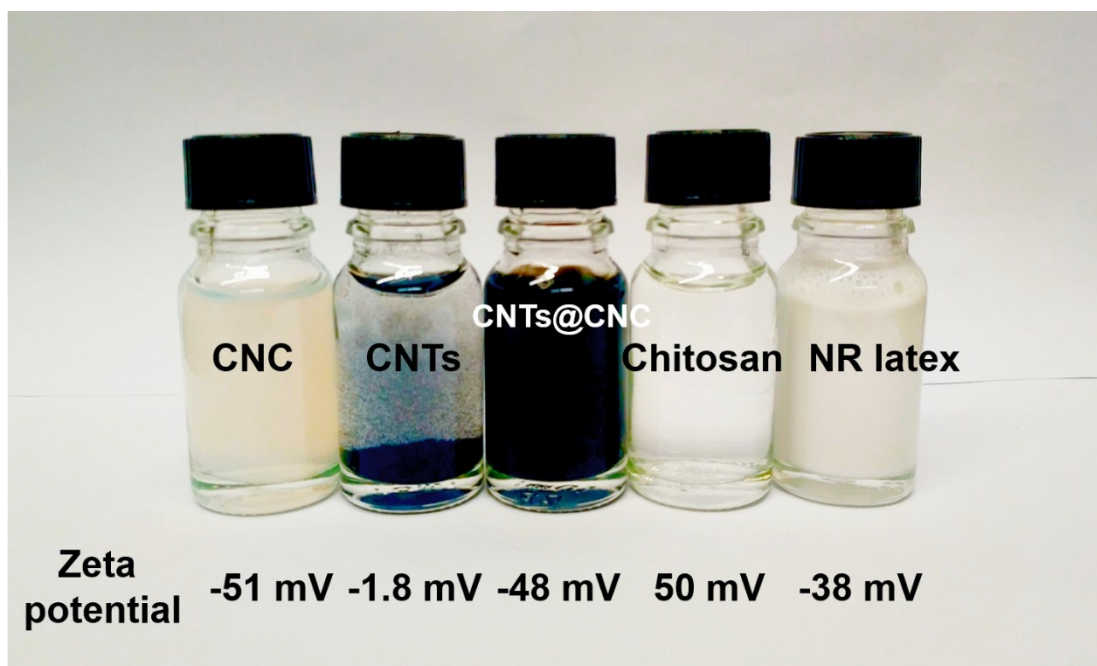
Figure S2. Images and Zeta potential values of CNC suspension, CNTs suspension, CNTs@CNC suspension, chitosan solution and NR latex, respectively.
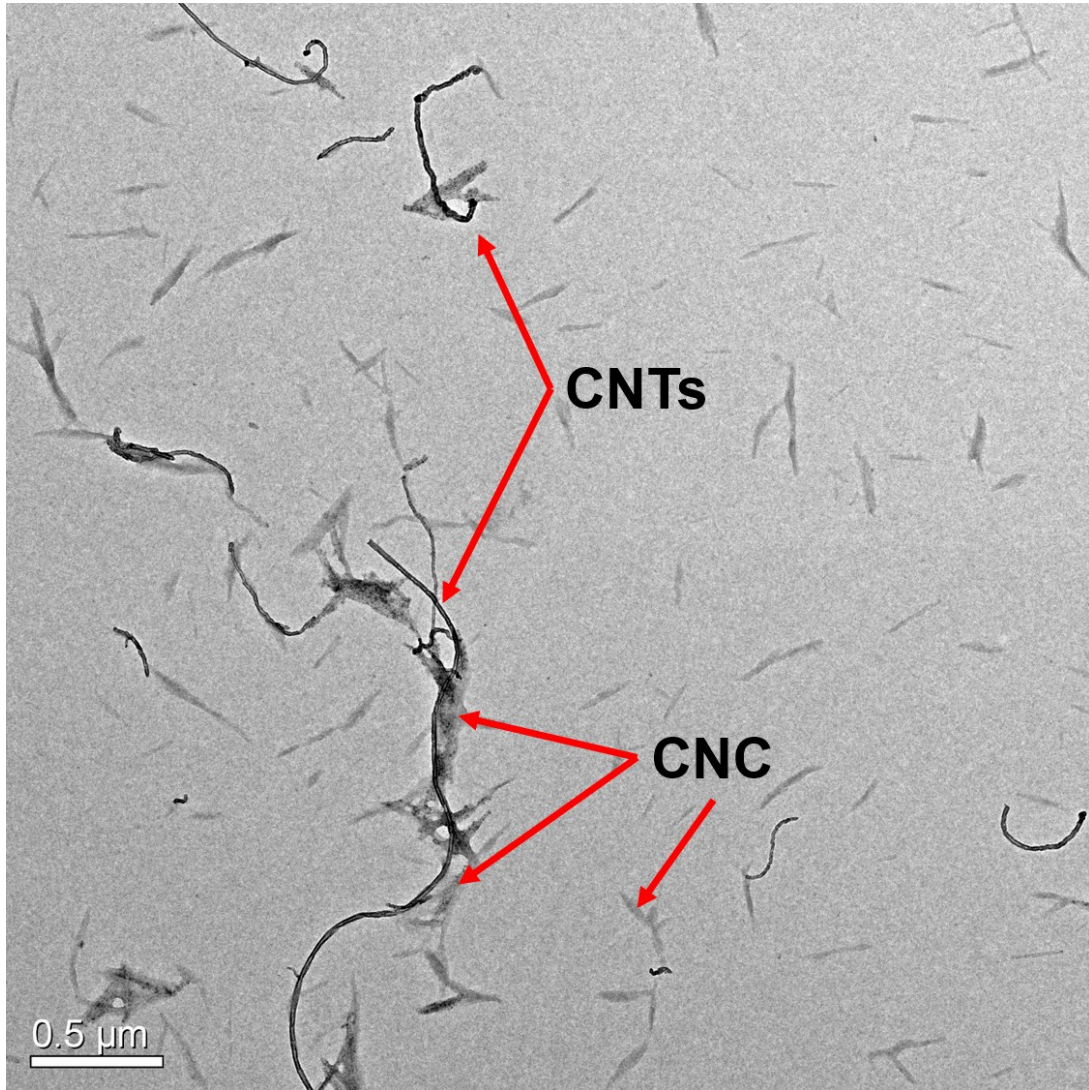
Figure S3. TEM image of CNTs@CNC nanohybrids.

The image shows that CNC is firmly attached and wrapped on CNTs, which greatly benefits the suspension stability of CNTs and is expected to facilitate the formation of a well-organized 3D segregated conductive network during the coagulation process.
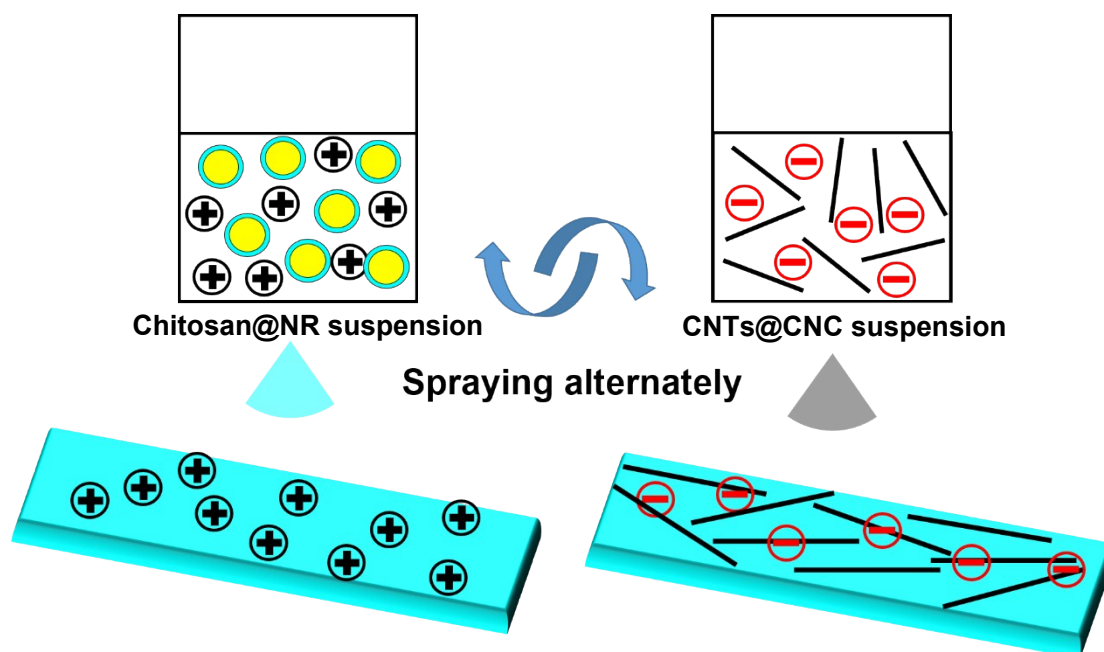
Figure S4. Schematic illustration for the fabrication of composites with "Mul" structure.

The zeta potential value of chitosan@NR suspension became 21.2 mV contrast to pure NR latex (-38 mV). For the "Mul" structure, the resistance largely depended on the mass ration of CNT and CNC. When CNT/CNC=1:1.5, the resistance of the samples is too large (>5 MΩ), and when CNT/CNC >1, CNTs cannot be dispersed steady.
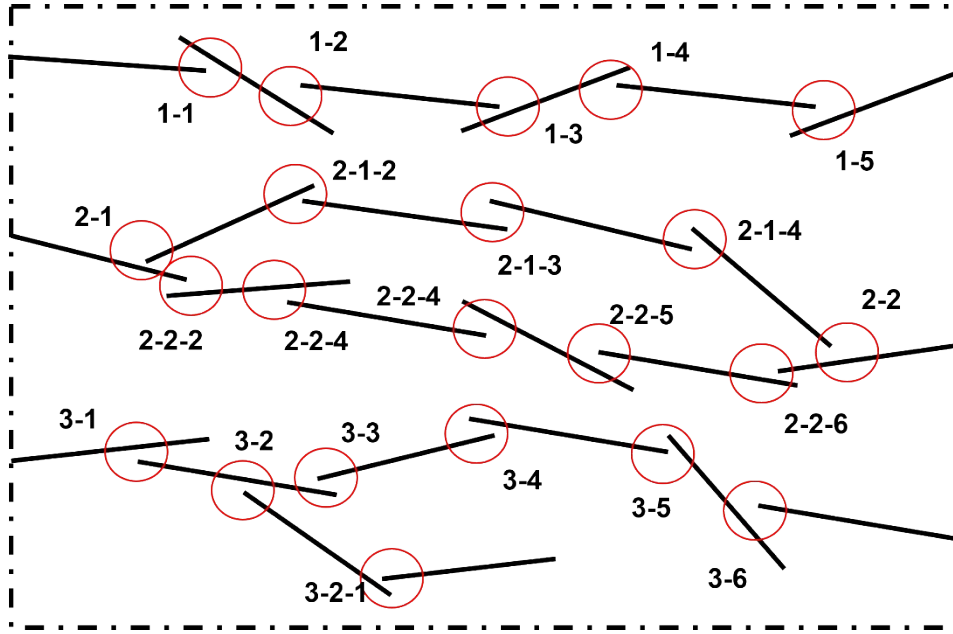
Figure S5. Schematic illustration for the calculation of conductive networks.

To construct the 3D resistor network model, for a CNTs with two contacting points (for example, 1-2 and 1-3) with neighboring CNTs, the resistance between these two points can be evaluated as:

$$R_{segment} = \frac{L_s}{\sigma * S}$$

Where R_S is the resistance of the conductive segment, L_S is the length between two points, σ is the electrical conductivity of CNTs (10^2 S/m, according to the specification of our CNTs) and r is the radius of CNTs (5 nm in this system). According to relative studies[2], the conductive network is mainly consist of CNTs connected by tunneling effect (resistance), where the tunneling resistance between two neighboring CNTs can be approximately estimated as:

$$Rtunnel = \frac{V}{A * J} = \frac{h^2 * d}{A * e^2 * \sqrt{2m\lambda}} exp(\frac{4\pi * d}{h} * \sqrt{2m\lambda})$$

Where V is the electrical potential difference, J is tunneling current density, A is the cross-sectional area of tunnel (10 nm*10 nm in this system, calculated by the radius of CNTs according to relative works[3]), h is Planck's constant, d is the tunnel distance

(calculated by the straight-line distance calculation tool in MATLAB), e is the quantum of electricity, m is the mass of electron, λ is the height of barrier (for CNTs, 5 eV in our system, determined according to relative standard papers in the field[2]). Now the resistance of conductive network is able to be quantitatively calculated based on these physics formulas. All the paths in the system were searched from the first carbon nanotubes to the last nanotubes (e.g. 1 to 1-1 and 2-1, and then 1-1 to 1-2, 2-1 to 2-2). The pathway consists of 1, 2-1, 2-2, 2-3 was set as isolated pathway and 1, 1-1, 1-2, 1-3, 1-4, 2 was regarded as pathway connect the beginning and the end. According to Kirchhoff's laws, the current of pathways connects the beginning and the end (for example, 1 to 2) was set as 1 A, and the current of isolated pathways was set as 0 A (for example, 1 to 2-3). Then we utilized the function for solving large sparse matrix (A*x=b) in Matlab to calculate the final result.

Here, as shown in **Figure S5**, we choose three representative conducting networks to demonstrate how the final resistance is calculated. The $R_{segment}$ is the resistance between two tunnle nodes, in which the distance can be calculated according to the coordinates of the nodes. To simplify the expression, the $R_{segment}$ represente the sum of the segment resistance of the whole conductive path, and R_{A-B} represent the corresponding R_{tunnel}. In the path 1, the resistans can be calculated as follows:

$$Rtotal = R_{1-1} + R_{1-2} + R_{1-3} + R_{1-4} + R_{1-5} + R_{segment}$$

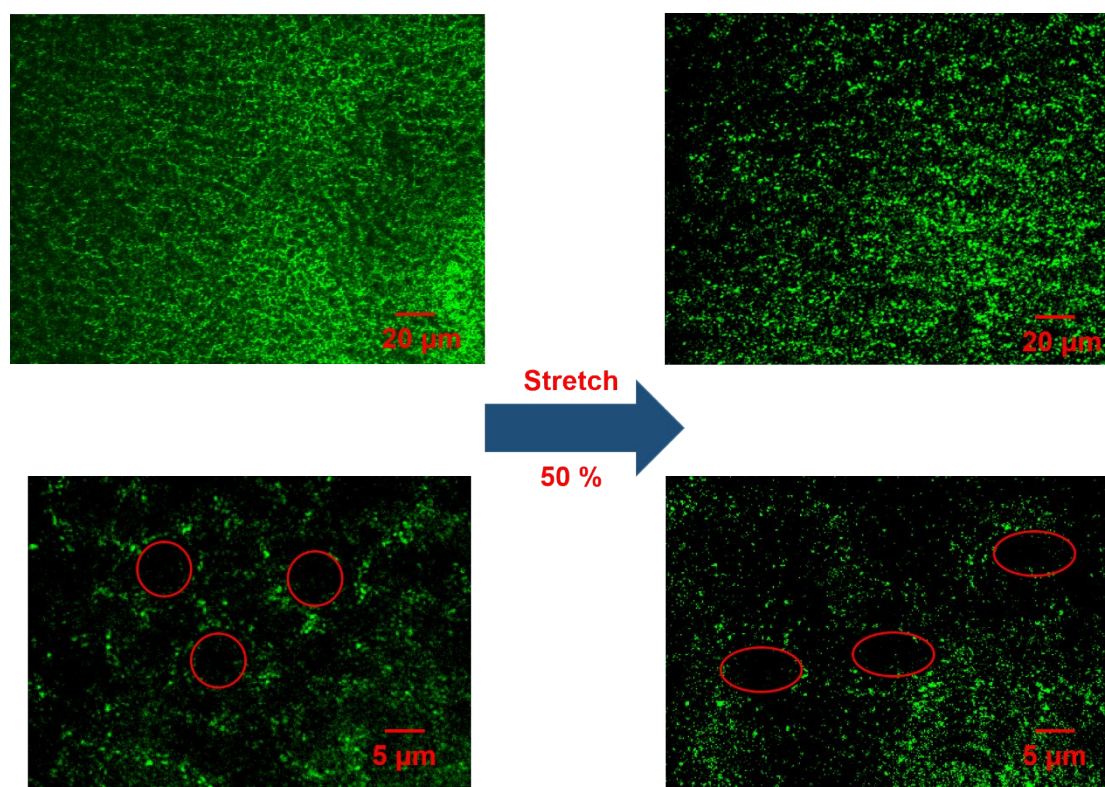In the path 2, the parallel circuit can be calculated as follows:

$$Rtotal = R_{segment} + \cfrac{1}{\cfrac{1}{R_{segment} + R_{2-1} + R_{2-1-2} + \ldots + R_{2-2}} + \cfrac{1}{R_{segment} + R_{2-2-2} + \ldots + R_{2-2-6}}}$$

In the path 3, there is a isolation pathway in which the current is set as 0 A, and the resistance is not involved in the calculation:

$$Rtotal = R_{3-1} + R_{3-2} + R_{3-3} + R_{3-4} + R_{3-5} + R_{3-6} + R_{segment}$$

Figure S6. LSCM images for the segregated nanostructure network variation of the sample under stretching at different magnification.

In order to intuitively observe the structural evolution of the nanostructured conductive network during stretching, laser scanning confocal microscope (LSCM) was carried out by means of labeling CNT@CNC nanohybrids with rhodamine 6G via physical absorption. To ensure the effective fluorescent labeling of CNT@CNC nanohybrids, 0.0004 g rhodamine 6G was dissolved in distilled water and mixed with 25 g obtained CNT@CNC suspension. And owing to the abundant functional groups and large specific surface area of CNT@CNC nanohybrids, the rhodamine 6G was absorbed on the surface of CNT@CNC nanohybrids after stirring for 30 min. Then, 0.18 g NR latex (solid content: 0.107 g) was added to the mixture and sonicated for 5 min to form a homogenous suspension. After removing the residual water quickly, an ultrathin film with segregated nanostructure network could be obtained for the LSCM measurement.

The rhodamine-labeled CNT/rubber nanocomposite was excited at 488 nm with a laser attenuation of 5 % and the emission light was recorded using band-pass filter to collect wave length between 500-700 nm. The LSCM images were taken at 200× magnification with a pinhole diameter of 1 Å. As shown in figure S6, a compact segregated nanostructure is clearly observed before stretching, and the deformation of rubber spheres (red circles) in CNTs reinforced rubber composite is well consistent with our calculation method (the size and shape of red circles are calculated according to the deformation mode of homogeneous rubber as illustrated in Figure S7).
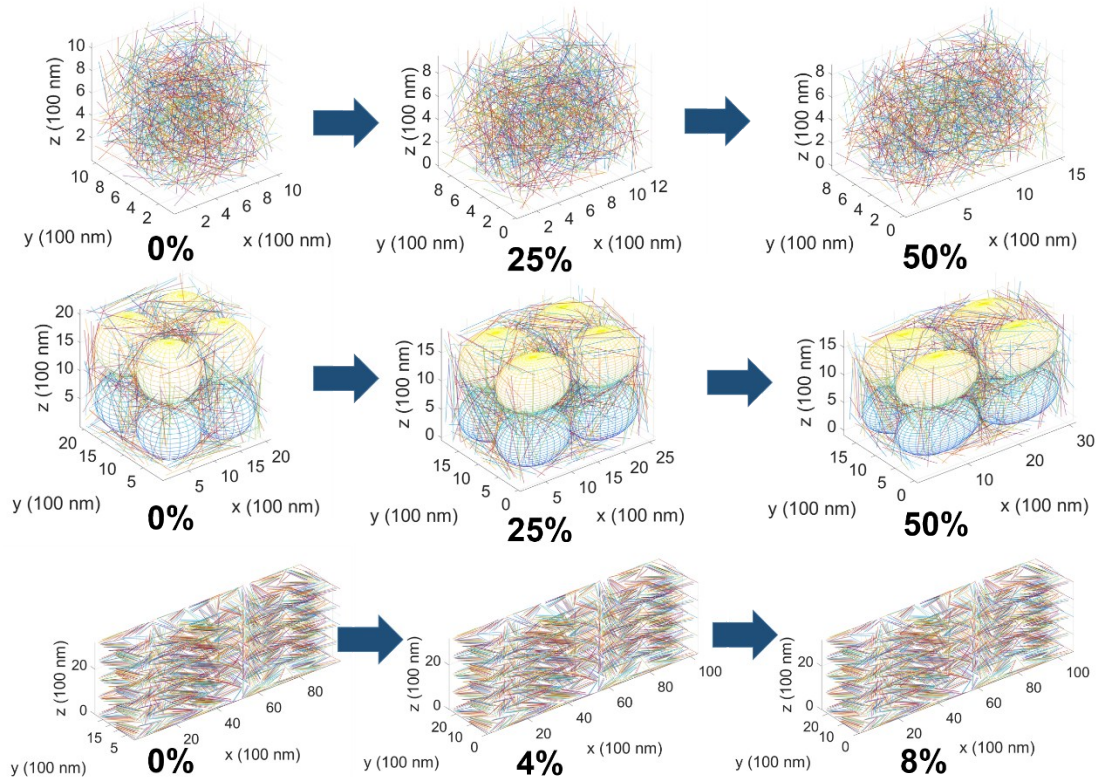
Figure S7. Schematic illustration for the deformation of different nanostructures under tensile strain.

For the deformation under tensile strain, as shown in **Figure 1b** and **S6**, the spatial position of CNTs change according to the deformation behaviour of rubber matrix, leading to a strain-induced structural evolution of conductive networks. The reorientation of CNTs under tensile strain in this system is simplified as a rigid-body movement due to a much higher Young's modulus of CNTs compared with rubber matrix. For natural rubber, the volume remains almost constant during stretching (Poisson's ratio is close to 0.5), and the coordinates changed from (x, y, z) to (a*x, b*y, b*z) where a and b are definite values calculated to ensure a constant volume of whole system. The system was
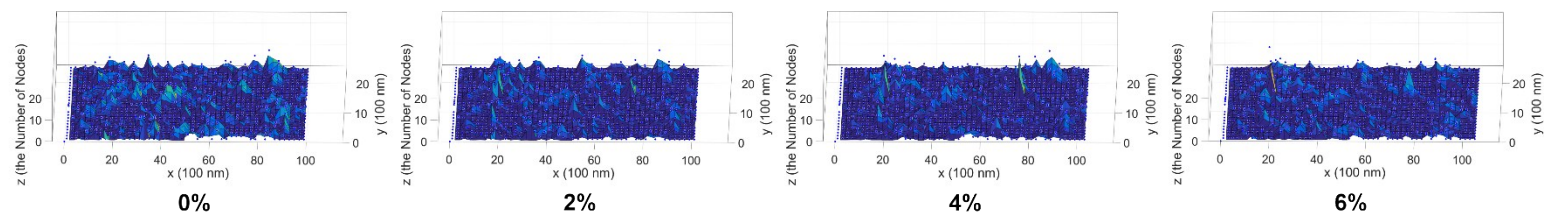
stretched based on this coordinate transformation while the length of CNTs kept

unchanged.
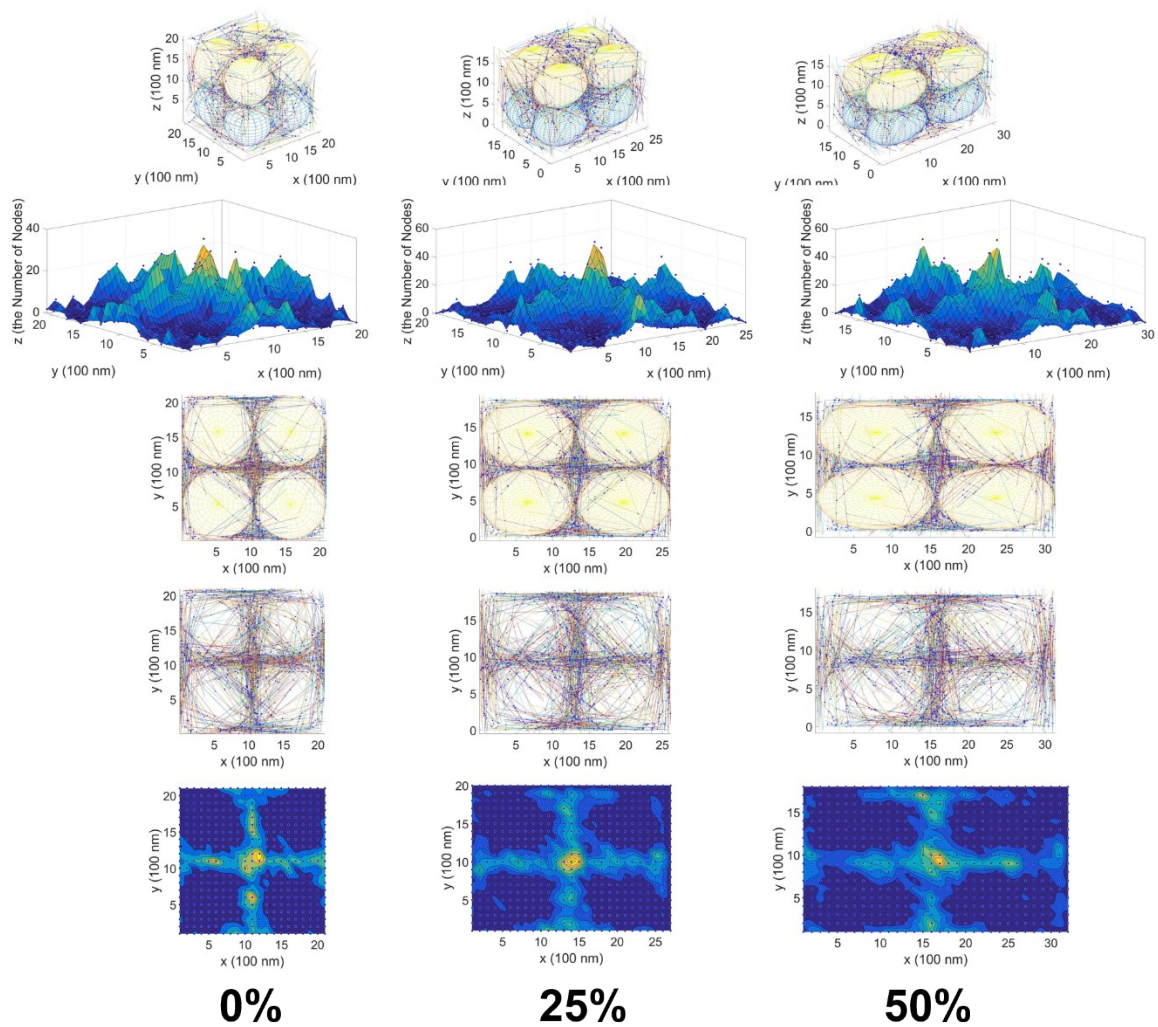
Figure S8. Schematic illustration for the deformation of "Seg" structure under tensile strain and corresponding visualized nodal analysis.
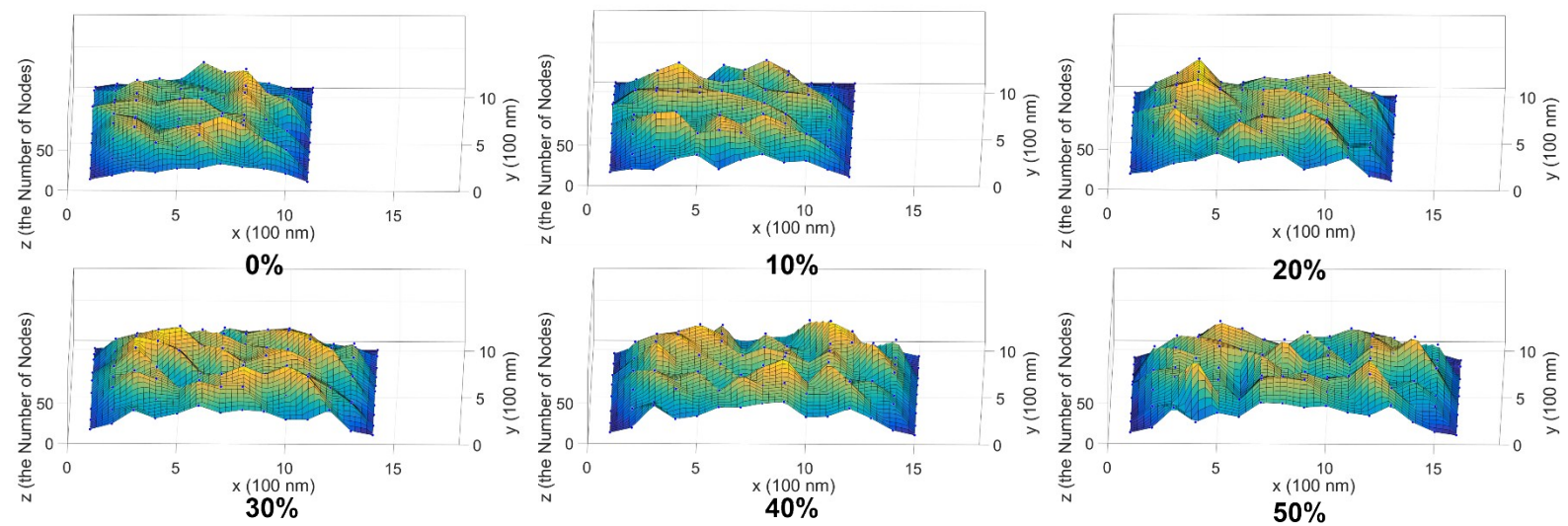
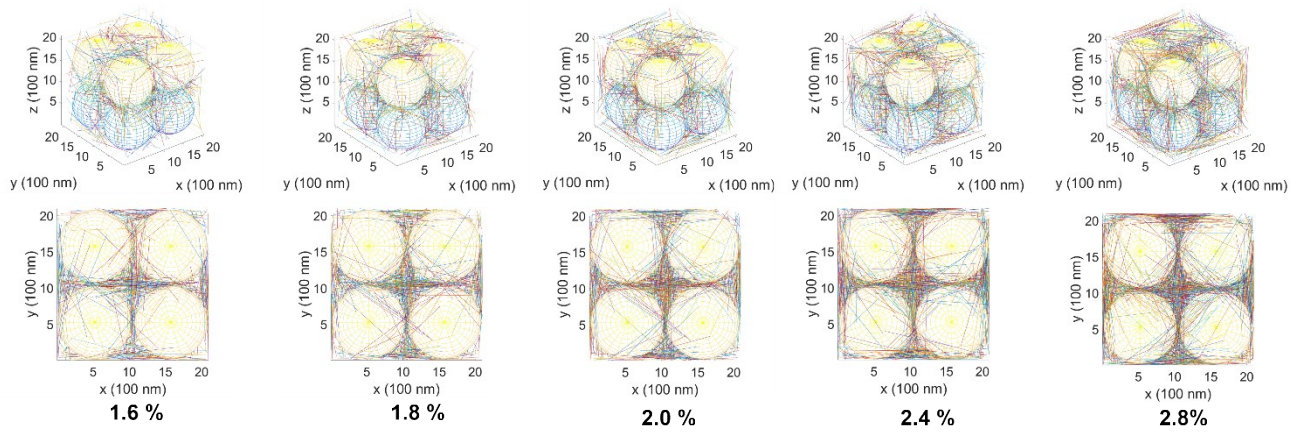**Figure S9**. The nodal dispersion plots of "Ran" structure under tensile strain.

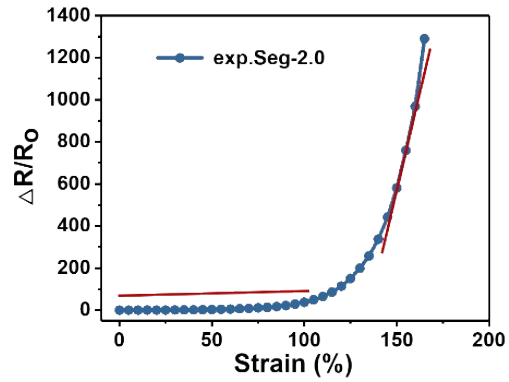**Figure S10**. The nodal dispersion plots of "Mul" structure under tensile strain.
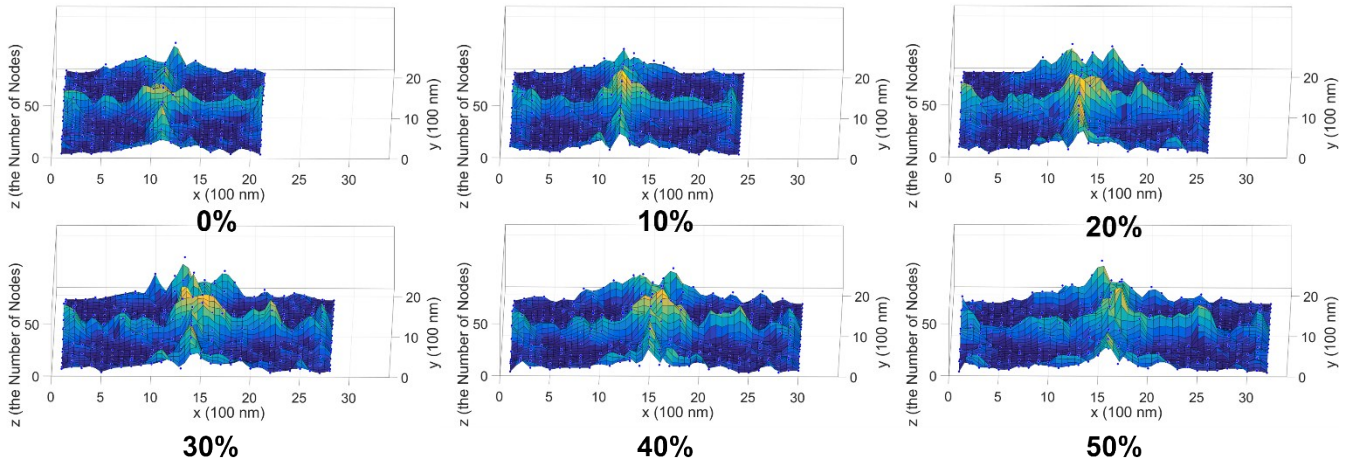
Figure S11. The nodal dispersion plots of "Seg" structure under tensile strain.

1.6 %   **1.8 %**   **2.0 %**   **2.4 %**   **2.8%**

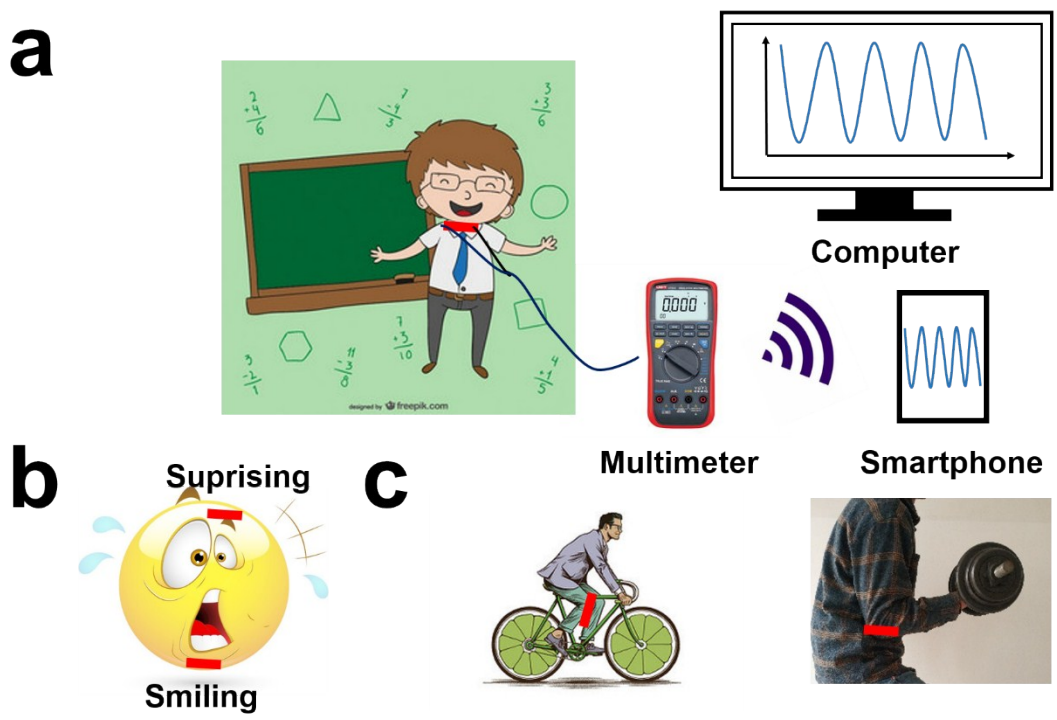**Figure S12**. Schematic illustration for the "Seg" structure with different CNTs' volume

fraction.

Figure S13. △R/R0-strain curve of "Seg-2.0".

Take the ΔR/R0-strain curve of "Seg-2.0" as an example, the curve can be roughly divided into two segments and which are approximately straight lines. The GF value are calculated as the slope of the fitting lines.

Figure S14. (a) Schematic illustration of the speech recognition based on our sensors. Schematic illustration of the test scenarios for expression recognition (b) and for human motion recognition (c).
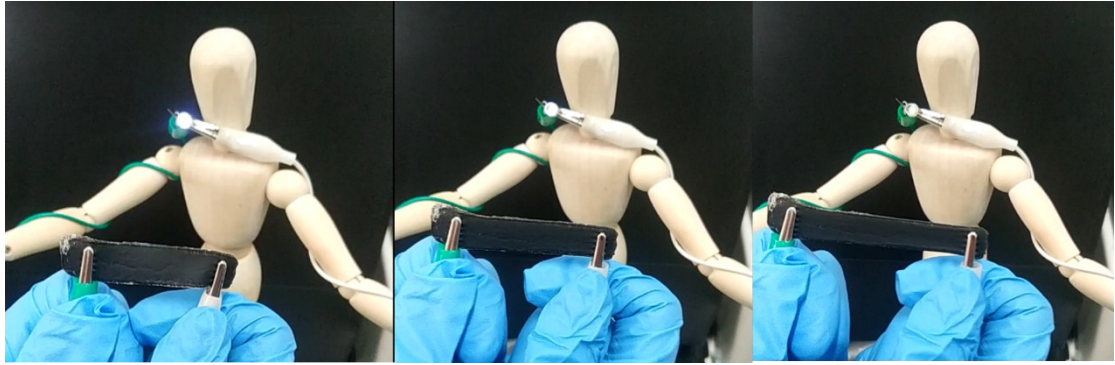
Figure S15. Application of "Seg-2.0" under large strain

The composites "Seg-2.0" can be used in the detection of large strain (> 100%) by simple and cheap system (such as a bulb), based on its high GF value under large strain.

Notes and references

1. W. S. Bao, S. A. Meguid, Z. H. Zhu, and G. J. Weng, *Journal of Applied Physics*, 2012, **111**, 093726.

2. N. Hu, Z. Masuda, C. Yan, G. Yamamoto, H. Fukunaga and T. Hashida, *Nanotechnology*, 2008, **19**, 215701.

3. C. Li, E.T. Thostenson, and T.-W. Chou, *Appl. Phys. Lett*, 2007, **91**, 223114.